In Situ Observation of the Formation of MoDTC-Derived Tribofilm on a ta-C Coating Using Reflectance Spectroscopy and its Effects on Friction

Naoya Hashizume[*a], Motoyuki Murashima[*a], Noritsugu Umehara[*a], Takayuki Tokoroyama[*a], Woo-Young Lee[*a]

[*a] Department of Micro-Nano Mechanical Science and Engineering, Nagoya University
Furo-cho, Chikusa-ku, Nagoya city, Aichi 464-8603, Japan
E-mail address of corresponding author: hashizume@ume.mech.nagoya-u.ac.jp

Abstract

We clarify the relationships between tribofilm thickness, chemical composition, and friction coefficient by combining *in situ* and *ex situ* analyses. An *in situ* reflectance observation is conducted for MoDTC-derived tribofilm on a ta-C coating during friction tests. The results show that the thicker the tribofilm is, the lower the friction coefficient. In addition, the refractive index increases as friction decreases. XPS analysis shows that the topmost surface of the thick tribofilm contains a higher MoS_2 concentration than the deep position. Therefore, the generated MoS_2-rich tribofilm is considered to reduce friction. In addition, as the MoS_2 tribofilm wears out, friction increases. In conclusion, we have developed a MoDTC-derived tribofilm formation model using a new method of *in situ* optical measurement.

Keywords: MoDTC; tribofilm; ta-C coating; *in-situ* reflectance observation

1. Introduction

Automobiles are widely used in modern society, and most of them have combustion engines. In addition, it is predicted that even in 2040, about 84% of automobiles, including hybrid vehicles, will have combustion engines [1-2]. Therefore, it is necessary to improve the efficiency of automotive combustion engines to reduce the consumption of fossil fuels and the emission of carbon dioxide. Friction loss in mechanical parts such as engines and transmissions accounts for almost 16.5% of the input energy of fuel [3]. Engine oil forms a film on sliding surfaces, decreasing friction. However, a thick oil film does not develop during slow-speed operation or in a stop sequence due to the lack of a hydrodynamic effect between surfaces in contact [4-5].

Additives in lubricant oil are quite important for reducing friction in boundary lubrication. One of the most commonly used additives is MoDTC (molybdenum dithiocarbamate), a friction modifier. MoDTC forms a thin tribofilm on friction surfaces. The tribofilm has a sheetlike structure consisting of MoS_2, which is widely used as a solid lubricant in industrial fields. The sheetlike MoS_2 allows surfaces to slide easily against each other, resulting in low shear force. Consequently, MoDTC reduces friction loss on sliding surfaces [6-10]. In addition, some researchers have tried to enhance the effects of oil additives. Taib *et al.* irradiated DLC coatings with ultraviolet rays and then conducted friction tests with additive-containing lubricants [11]. As a result, the UV-irradiated DLC coatings formed thicker tribofilms on wear tracks, and the tribological properties of the DLC coatings were improved. Therefore, the thickness of the tribofilm significantly affects the

tribological properties in boundary lubrication conditions.

DLC (diamondlike carbon) coatings are also considered promising tribomaterials for reducing friction loss in boundary lubrication conditions. DLC is an amorphous material consisting of C-Csp^2 bonding and C-Csp^3 bonding. Because the nature of the carbonaceous structure includes both graphitelike and diamondlike structures, DLC coatings show excellent low-friction and high-wear-resistance properties [12-15]. Due to the increased application of DLC coatings, the effects of MoDTC additives on the tribological characteristics of DLC coatings need to be clarified. For example, some researchers have reported that MoDTC accelerates the wear of a-C:H (hydrogen-containing amorphous carbon) coatings and have proposed mechanisms underlying accelerated wear [9-10]. In terms of the friction coefficient, MoDTC shows excellent low friction on ferrous mechanical parts. However, some researchers have reported that MoDTC is inactive in DLC coatings, diminishing the low friction effect [16]. On the other hand, another report has shown that thick MoDTC-derived tribofilm can form on DLC coatings, reducing friction due to the rich MoS_2 [17]. In conclusion, to clarify the formation behavior of MoDTC-derived tribofilm, we developed an *in situ* observation method to reveal dynamic changes in tribofilm formation.

Recently, to break through the limitations of *ex situ* analysis, some researchers have developed *in situ* observation methods to perform during friction tests. Okubo et al. and Xu et al. developed *in situ* Raman observation devices. In both cases, the authors used Raman spectroscopy to evaluate the amount of MoS_2 in tribofilm [18-20]. However, neither of those methods can measure tribofilm thickness. Optical *in situ* observation is quite effective at providing a transition for surfaces in contact with each other [21-23]. In addition, some researchers have developed optical *in situ* observation methods using reflectance spectroscopy. Such methods are not only nondestructive forms of observation but also measure characteristics of tribofilm (i.e., thickness, refractive index n, and extinction coefficient k). It is well known that the thickness of a tribofilm strongly affects friction and wear properties. In addition, the refractive index and extinction coefficient are consistent with the density and sp^2 fraction, respectively. Nishimura et al. have revealed that the friction coefficient depends on both the thickness and hardness (consistent with a refractive index) of a tribofilm [24,25]. In addition, several researchers have shown that an increase in the Van deer Waals force estimated from the reflectance leads to a decrease in the friction coefficient [26,27]. And the method using the reflectance spectroscopy has revealed the complicated hydrodynamic lubrication conditions in two-phase lubricants [28]. In conclusion, an *in situ* observation method using reflectance can have the potential to reveal the formation behavior of MoDTC-derived tribofilms on DLC coatings.

In the present paper, we clarified the formation behavior of MoDTC-derived tribofilm on a ta-C coating. We also revealed the relationships between tribofilm characteristics and the friction coefficient. We then presented X-ray photoelectron spectroscopy (XPS) analysis to revealed chemical composition of the MoDTC-derived tribofilm (i.e., amount of MoS_2). Consequently, we developed a new mechanism of tribofilm formation on the ta-C coating, based on the results of *in situ* and *ex situ* surface analysis.

2. Experiments

2.1. Specimen

We prepared a ta-C coating and deposited it on Si<100> wafers. Nanoindenter equipment (ENT-1100a, Elionix, Japan) measured the hardness and Young's modulus of the ta-C coating, which were 24.9 GPa and 284 GPa, respectively. The coating thickness of 112 nm was measured using reflectance spectroscopy (OPTM-H2, Otsuka Electronics Co., Ltd., Japan). An atomic force microscope (SPM-9700, Shimadzu Corporation, Japan) measured the roughness of the ta-C coating; the root mean square roughness R_q was 7.1 nm.

A sapphire hemisphere was used as a mating material in the friction test. The hardness and Young's modulus of the sapphire hemisphere were 22.5 GPa and 470 GPa, respectively, and R_q was 4.0 nm. The transmittance of the sapphire hemisphere for visible light was more than 85%. Therefore, the sapphire hemisphere did not prevent the measurement of reflectance.

2.2. Pin-on-disk friction test with *in situ* reflectance spectroscopy

Figure 1 shows a pin-on-disk friction tester with the *in situ* reflectance spectroscopy. The reflectance spectroscopy measured the reflectance light from the friction area through the sapphire hemisphere. The measuring light irradiated the contact point via the sapphire hemisphere. The diameter of the measuring point was 10 μm, which was smaller than the Hertzian contact diameter of 40 μm. We conducted friction tests at a normal load of 0.5 N, a temperature of 80 ºC, and a sliding speed of 12.6 mm/s (rotation radius of 2 mm and 60 rpm) (see Table 1). The friction tests stopped after 1800 cycles of sliding, and then surface analyses (e.g., XPS and optical microscope measurement) were conducted. We used poly-α-olefin 4 (PAO4) as an oil lubricant with a 700 ppm MoDTC concentration. This lubricant had a viscosity of 3.75×10^{-3} Pa·s at 80 ºC and a viscosity-pressure coefficient of 11.0 GPa^{-1}. The oil thickness ratio Λ under the friction test was 0.11, resulting in boundary lubrication conditions [4]. Reflectance from 360 nm to 800 nm wavelength was measured every 10 cycles.

Table 1 Friction test conditions

ta-C coating *vs.* Sapphire hemisphere	
Normal load	0.5 N
Temperature	80 °C
Sliding cycles	1800
Sliding speed	12.6 mm/s
Average Hertzian contact pressure	405 MPa
Film thickness ratio	0.11

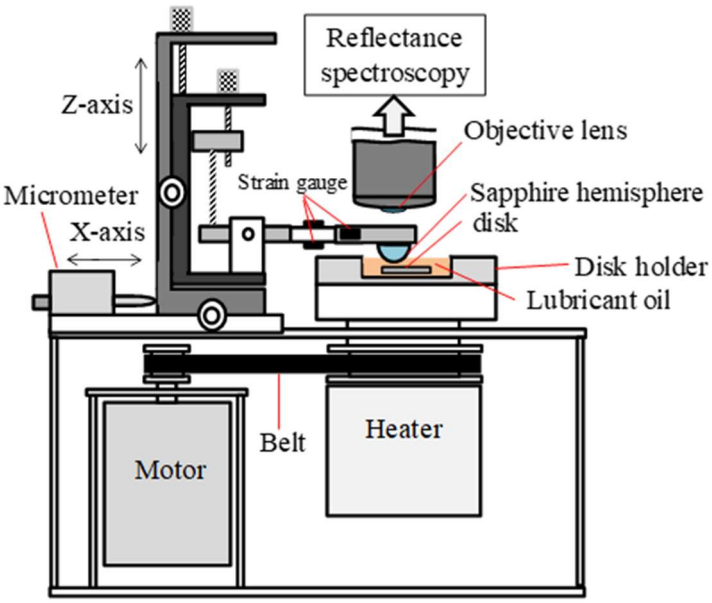

Fig. 1 A schematic of the pin-on-disk friction tester with reflectance spectroscopy

2.3. Reflectance fitting

We conducted the reflectance fitting to calculate the thickness and optical properties of the friction area using OPTM post-analysis software (Otsuka Electronics Co., Ltd., Japan). Reflectance measured by reflectance spectroscopy was calculated using Eq. (1).

$$R = \frac{\text{Intensity of reflected light}}{\text{Intensity of incident light}} \tag{1}$$

Figure 2 shows the optical model of the friction area. In the model, the substrate and atmosphere were Si and sapphire, respectively. The analysis layers were the tribofilm derived from MoDTC, the transformed layer of the ta-C coating, and the as-deposited ta-C coating. In the experimental condition, the oil film thickness was 0.8 nm as calculated by the Hamrock−Dowson formula, which was less than the 1 nm minimum resolution of reflectance spectroscopy [4]. Therefore, the oil film was not considered in the optical model. From Fig. 2, the reflectance of the optical model R_{01234} was calculated by Eqs. (2)-(8) [29].

$$R_{01234} = |r_{01234}|^2 \tag{2}$$

$$r_{01234} = \frac{r_{01}+r_{1234}\exp(-i2\beta_1)}{1+r_{01}r_{1234}\exp(-i2\beta_1)} \tag{3}$$

$$r_{1234} = \frac{r_{12}+r_{234}\exp(-i2\beta_2)}{1+r_{12}r_{234}\exp(-i2\beta_2)} \tag{4}$$

$$r_{234} = \frac{r_{23}+r_{34}\exp(-i2\beta_3)}{1+r_{23}r_{34}\exp(-i2\beta_3)} \tag{5}$$

$$N_m = n_m - ik_m \quad (m = 0,1,2,3,4, N_m, n_m \text{and } k_m \text{ depend on wavelength } \lambda) \tag{6}$$

$$r_{ij} = \frac{N_i\cos\theta_i - N_j\cos\theta_j}{N_i\cos\theta_i + N_j\cos\theta_j} \qquad (i = 0,1,2,3,\ j = 1,2,3,4) \tag{7}$$

$$\beta_m = \frac{2\pi t_m N_m \cos\theta_m}{\lambda} \quad (8)$$

r_{ij} is the amplitude reflectivity between the interface of i and j, β_m is the interference phase angle, N_m, n_m, and k_m are the complex refractive index, the refractive index, and the extinction coefficient of each layer, respectively. t_m is the thickness of each layer. Suffixes 0, 1, 2, 3, and 4 indicate sapphire, the tribofilm derived from MoDTC, the transformed layer of the ta-C coating, the as-deposited ta-C coating, and the Si substrate, respectively. The calculated reflectance R_{01234} (Eqs. (2)-(8)) was fitted to the measured reflectance R (Eq. (1)) using the nonlinear least-squares method, and then the thickness t, the spectrum of refractive index n, and extinction coefficient k of each layer were determined. In the optical model, we assumed a series of a single layer. To design the optical model, we referred to the effective medium approximation. From that approximation, we could treat the layer that included the material with different properties as one simple layer and then get the average optical properties and thickness of the layer. Therefore, it was reasonable to treat each layer as a perfect layer to get the average data of the measured spot. This optical model for the fitting of the friction test with MoDTC-added lubricant is verified in section 4.

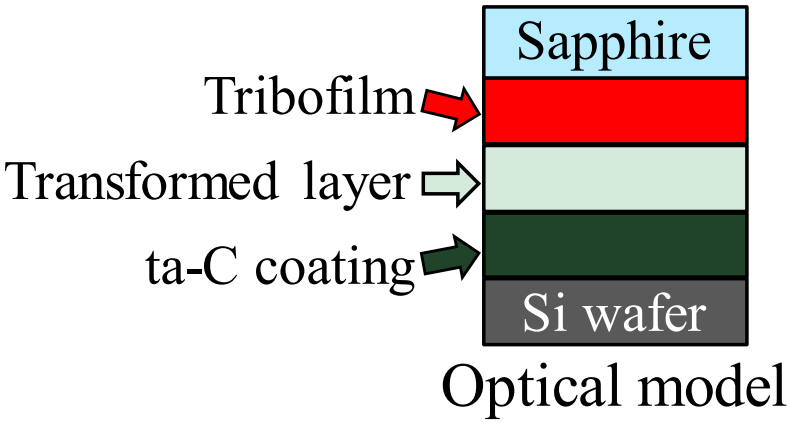

Fig. 2 Optical model of the friction point for the reflectance fitting

2.4. X-ray Photoelectron Spectroscopy

We analyzed the composition of the MoDTC-derived tribofilm using XPS (PHI Quantera III, ULVAC-PHI Inc., Japan). This device had a spot diameter of 100 μm. Ar-ion sputtering was conducted to eliminate contamination of the top surface and to obtain depth profiles. We obtained the narrow spectra of Mo3d and S2p peaks. Each obtained spectrum shifted by the effect of charging. Therefore, each spectrum was calibrated by the Ar2p peak position (241.9 eV). Peak fitting and deconvolution were conducted with the Shirley algorithm to remove the background and Gaussian−Lorentzian mixed function to separate the peaks from each other. Table 2 shows the fitting condition for the Mo3d peak [30-35]. Table 3 shows the fitting condition for the S2p peak [36,37]. Figure 3 shows an example of peak deconvolution of the Mo3d peak.

Table 2 Conditions of the peak deconvolution of Mo3d peaks

Peak Number	(1)	(2)	(3)	(4)	
Peak name	Mo(0), Mo^{2+}	Mo(0), Mo^{2+}	Mo^{4+}	Mo^{4+}	
Orbit	3d 5/2	3d 3/2	3d 5/2	3d 3/2	
Compounds	Mo, Mo_2C	Mo, Mo_2C	MoS_2, MoO_2	MoS_2, MoO_2	
Gaussian ratio [%]	80	80	80	80	
Position [eV]	228.0±0.2	(1)+3.13	229.4±0.2	(3)+3.13	
Area ratio	-	(1)×2/3	-	(3)×2/3	
FWHM ratio	-	Same as (1)	-	Same as (3)	
Peak Number	(5)	(6)	(7)	(8)	(9)
Peak name	Mo^{5+}	Mo^{5+}	Mo^{6+}	Mo^{6+}	S^{2-}
Orbit	3d 5/2	3d 3/2	3d 5/2	3d 3/2	2s
Compounds	MoDTC	MoDTC	MoO_3	MoO_3	-
Gaussian ratio [%]	80	80	80	80	80
Position [eV]	231.0±0.2	(5)+3.13	232.6±0.2	(7)+3.13	228.0±0.3
Area ratio	-	(5)×2/3	-	(7)×2/3	-
FWHM ratio	Same as (3)	Same as (3)	-	Same as (7)	-

Table 3 Conditions of the peak deconvolution of S2p peaks

Peak Number	(1)	(2)	(3)	(4)
Peak name	S-S	S-S	Mo-S	Mo-S
Orbit	2p 3/2	2p 1/2	2p 3/2	2p 1/2
Compounds	S	S	MoS_2	MoS_2
Gaussian ratio [%]	80	80	80	80
Position [eV]	164.0±0.2	(1)+1.18	161.6±0.2	(3)+1.18
Area ratio	-	(1)×1/2	-	(3)×1/2
FWHM ratio	-	Same as (1)	-	Same as (3)

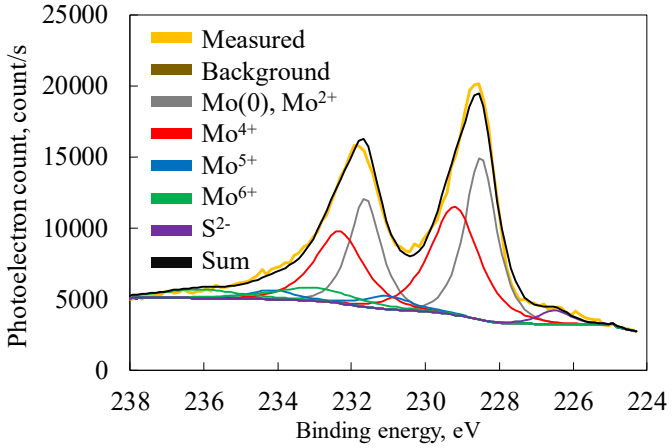

Fig. 3 Example of peak deconvolution of XPS analysis

3. Friction test and post-test surface observation

We conducted friction tests of 1800 cycles under the conditions shown in Table 1. We compared the friction test results of MoDTC-added base oil and pure base oil to evaluate the friction-reduction effect of MoDTC. Figure 4 shows the raw data of the friction coefficients with different lubricants. The black and red lines indicate the MoDTC-added base oil and the pure base oil, respectively. In the initial 180 cycles, the average friction coefficient of the MoDTC-added PAO4 was lower than that of pure PAO4 by 8.4%. This indicated that the addition of MoDTC reduced the friction of the ta-C coating even in the initial stage of the friction test. After 180 to 1800 cycles, the friction coefficient of the MoDTC-added base oil decreased to 0.13, which was 12.5% lower than that of the pure base oil. Thus, the addition of MoDTC contributed to the reduction of the friction coefficient in all stages of the friction test. In addition, the friction of MoDTC-added PAO4 at the last stage of the test was remarkably low. In the last 180 cycles, the average friction coefficient of MoDTC-added lubricant was 0.10, which is approximately 40% lower than that of the pure base oil. Espejo et al. reported that the friction coefficient of MoDTC-added oil was reduced to around 0.03 in a steel/ta-C tribosystem, which was approximately half the friction coefficient of the pure base oil [9]. In our experiment, the friction coefficient of MoDTC-added oil also decreased compared to the friction coefficient of the pure base oil. However, in our experiment, the friction coefficient decreased to around 0.10 and was thus three times that of the steel/ta-C system. We conducted the friction test in a sapphire/ta-C system, which may have caused such a difference in friction reduction.

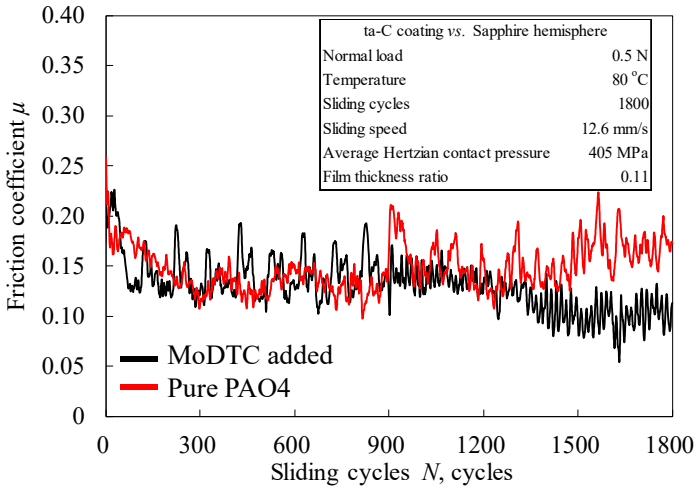

Fig. 4 Raw data of the friction coefficients with MoDTC-added base oil and pure base oil

After the friction test, we observed the wear track using an optical microscope (BX60M, Olympus Corporation, Japan). We are able to see the adhesion material in the wear track of the MoDTC–added lubricant (Fig. 5a). The adhesion material shown in Fig. 5a was only observed on the ta-C coating, not the mating material of the sapphire hemisphere. On the other hand, there is no tribofilm in both the wear track of the pure

PAO4 (Fig. 5b) and the sapphire hemisphere. Therefore, the presence of MoDTC-derived tribofilm may result in the reduction in the friction coefficient. Fig. 6a and Fig. 6b compare the detail morphology of the wear tracks of the MoDTC-added lubricant and the pure PAO4 lubricant. In Fig. 6a, tribofilm was adhered on the ta-C coating and its thickness was 56.9 nm. On the other hand, the wear track of the pure PAO4 oil was relatively smooth, and the adhesion material shown in Fig. 6a was not observed in Fig. 6b. From the surface observation, the formation of the tribofilm was particular to MoDTC-added lubricant. Therefore, the adhesion material in Fig. 5a and Fig. 6a can be considered as the MoDTC-derived tribofilm.

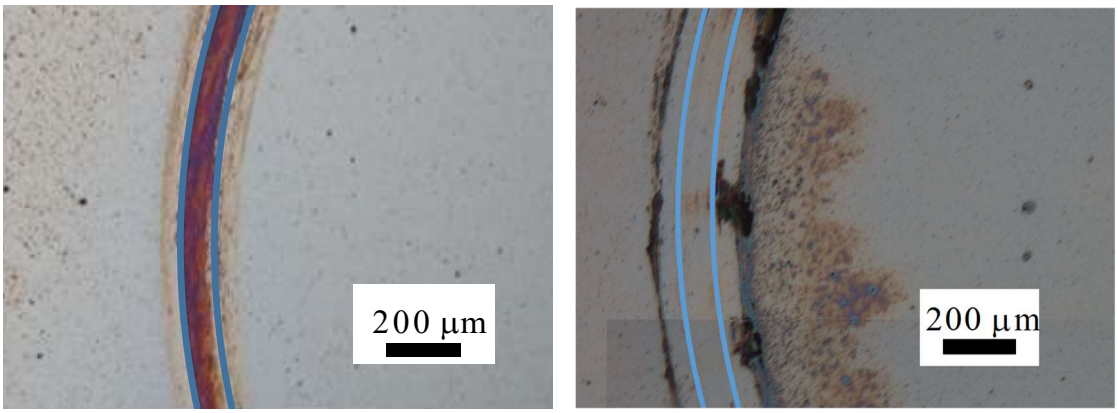

Fig. 5 Optical microscope images of the wear tracks of (a) MoDTC-added base oil and (b) pure base oil

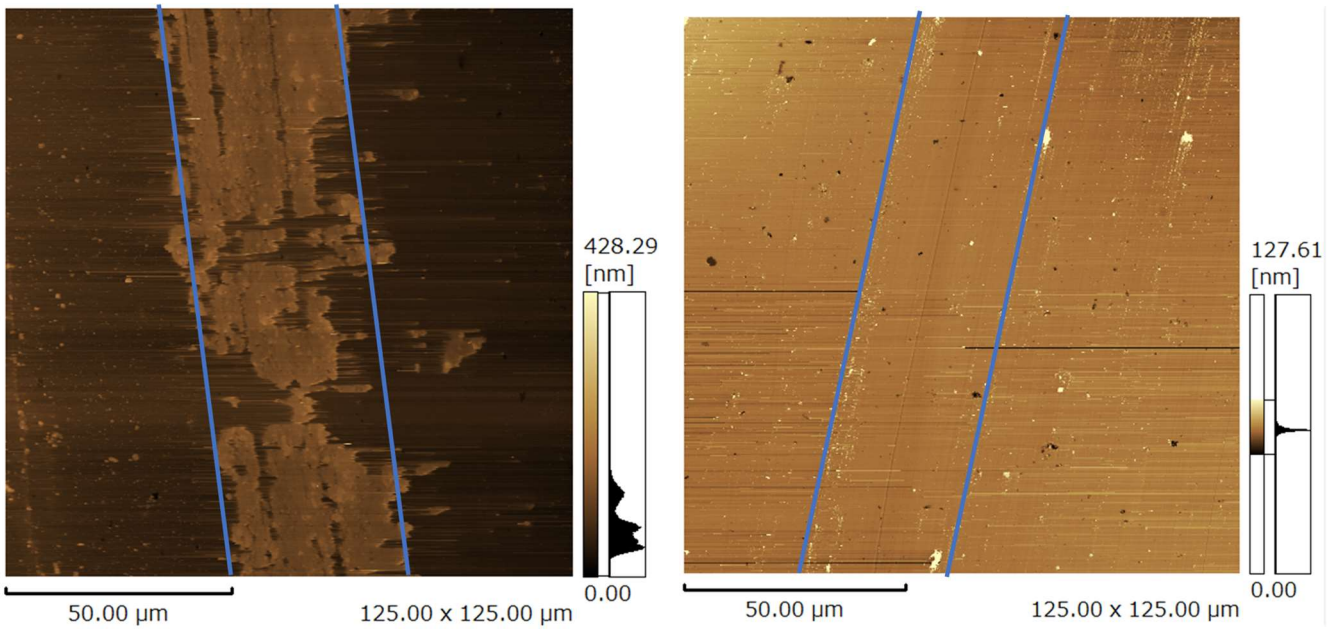

Fig. 6 AFM images of the wear tracks of (a) MoDTC-added base oil and (b) pure base oil

In addition, we observed the sapphire hemisphere by AFM and obtained the surface roughness after the friction test revealing an increase in the surface roughness on the order of a few nanometers (R_q of 15.5

nm). On the other hand, this value indicated that the boundary lubrication state was maintained throughout the friction test, which is also important for deciding the optical model to conduct the reflectance fitting. We developed an optical model of the contact point (Fig. 2) due to the severe contact state. Therefore, we considered that we were able to use the same optical model shown in Fig. 2 because the severe contact state was maintained throughout the friction test.

We reported that the friction coefficient was reduced when MoDTC was added to the base oil, and we observed the MoDTC-derived tribofilm by an optical microscope. Komori et al. reported that the friction reduction effect of MoDTC increased when they used rough specimens [38,39]. This is due to the increase in local contact pressure on the rough contact surface, resulting in greater energy on the contact surface, which enhanced the generation of MoS_2. Considering the previous research, the increase in surface roughness reduced the friction coefficient in our experiment due to the MoS_2 formation. In the next section, we show the results of the *in situ* reflectance observation and then clarify the relationship between the MoDTC-derived tribofilm and the friction coefficient.

4. *In situ* observation result of the friction test

The friction test result with the MoDTC-added lubricant shown in Fig. 4 revealed that the friction coefficient started decreasing from the 900th cycle. Interestingly, the coefficient fluctuated severely from 100 to 900 cycles. The fluctuation of the friction coefficient is considered to come from the characteristics of the tribofilm. To evaluate tribofilm formation during the friction test, we analyzed the reflectance spectrum of the friction surface during the friction test. Figure 7 illustrates the spectrum shift from 300 to 640 sliding cycles. Every spectrum had a peak at 470 nm, although they had different curvatures, indicating differences in the composition and thickness of the tribofilm. We also show the results of the reflectance spectrum of the friction test with the pure PAO4 lubricant (Fig. 8), revealing the spectrum shift from 300 to 640 sliding cycles.

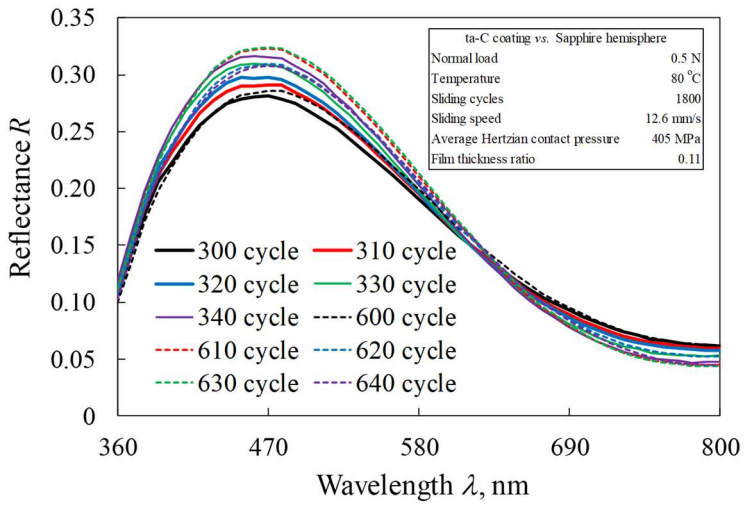

Fig. 7 *In situ* measurement results of reflectance spectra of the friction test with MoDTC-added base oil

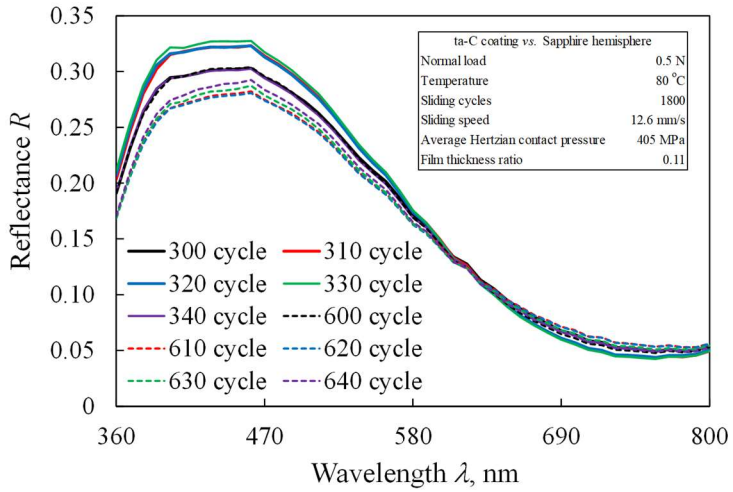

Fig. 8 *In situ* measurement results of reflectance spectra of the friction test with pure base oil

From the reflectance fitting for the friction test with pure PAO4, an oil film with a thickness of approximately 1 nm formed, which was close to the 0.8 nm oil film thickness calculated by the Hamrock−Dowson formula. The 1 nm oil film thickness is almost the minimum resolution of the optical analysis. Therefore, for the convergence and computational power saving, we used the optical model without the oil film, which did not affect the analysis result. In addition, the transformed layer of the ta-C coating formed on the topmost layer. The extinction coefficient of the transformed layer at the wavelength of 589 nm was 2.28, which was larger than the 1.00 value of the as-deposited ta-C coating. The increase in the extinction coefficient indicated the graphitization of the as-deposited ta-C coating. The result of the reflectance fitting of the friction test with the pure PAO4 lubricant indicated the presence of the transformed layer of the DLC coating due to friction.

We conducted the reflectance fitting of the MoDTC-added lubricant. Considering the reflectance fitting for the friction test with the pure PAO4 lubricant, we assumed the existence of the transformed layer of the ta-C coating. To reduce the amount of calculation, the optical properties of the transformed layer were fixed. Figure 9 shows the relationship between the thickness of the tribofilm and the friction coefficient. At the last stage of the friction test, the thickness of the tribofilm was 57.2 nm, which was extremely close to the 56.9 nm obtained by AFM observation. Therefore, we considered the result of the reflectance fitting reasonable. The thickness fluctuates severely from 100 to 900 cycles. The duration matches the fluctuating period of the friction coefficient. Interestingly, the film thickness decreased at the same time as the increase in the friction coefficient. This result strongly indicated that the thicker MoDTC-derived tribofilm was very important for achieving low friction. In the period from 900 to 1800 cycles, the tribofilm thickness evolved in a different way: it increased with the number of sliding cycles, consistent with the decrease in the friction coefficient. Figure 10 shows a scatter graph of the tribofilm thickness and the friction coefficient. The figure clearly indicates that the friction coefficient decreased with an increase in the thickness of the tribofilm. To quantify

the effect of tribofilm thickness on the friction reduction, we introducef the correlation coefficient R, which is determined by Eq. (9) [40].

$$R = \frac{s_{xy}}{s_x s_y} \tag{9}$$

s_x and s_y are standard deviations of the tribofilm thickness and the friction coefficient, respectively. s_{xy} is the covariance between the tribofilm thickness and the friction coefficient. $|R| = 1$ indicates a complete relation. $0.7 \leq |R| < 1$ indicates a relatively strong. The analysis result showed a strong correlation between the tribofilm thickness and the friction coefficient ($R = -0.732$). From this result, we can infer that the thickness of the tribofilm significantly affected the friction coefficient.

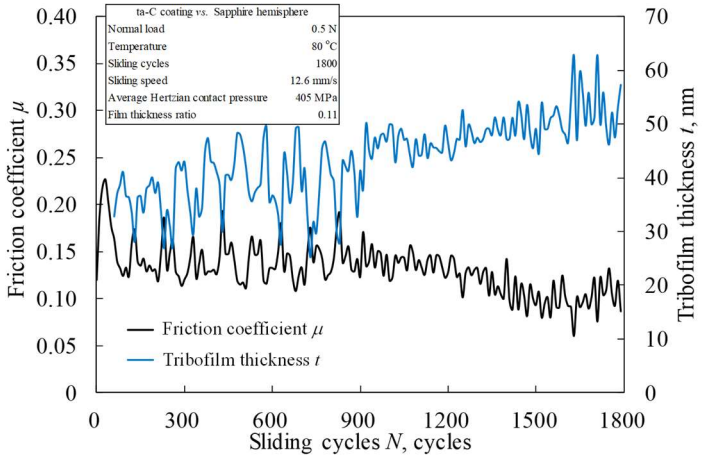

Fig. 9 The evolution of the relationship between the thickness of MoDTC-derived tribofilm and the friction coefficient

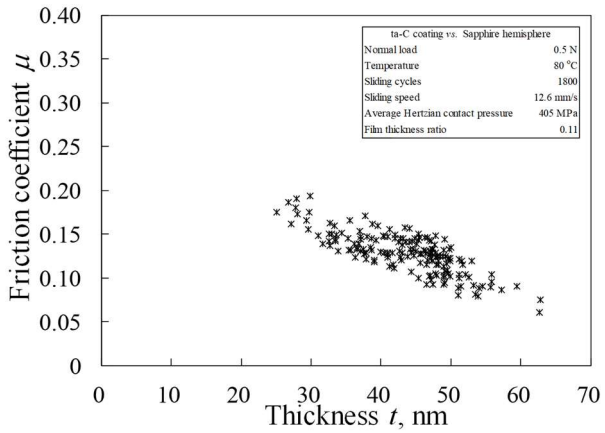

Fig. 10 Scatter graph of the thickness of MoDTC-derived tribofilm and the friction coefficient

The evolution of the relationship between the refractive index n and the friction coefficient is shown in Fig. 11. The refractive index also fluctuated from 100 to 900 cycles, like both the friction coefficient and the refractive index. Optical properties (refractive index n and extinction coefficient k) were unique to each tribological product. Therefore, the result led to an interesting consideration, which was that the generated tribofilm on the topmost surface had a different chemical composition than the lower layer. In addition, the fluctuation of the refractive index was suppressed at the higher position after 900 cycles, where the friction coefficient also started showing a straight-decrease tendency. The extinction coefficient showed similar behavior, consistent with the friction fluctuation (Fig. 12).

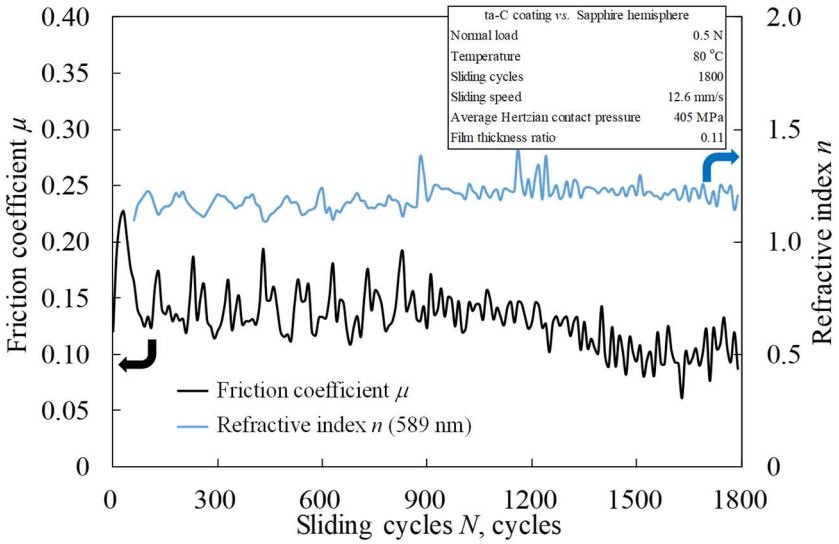

Fig. 11 Evolution of the refractive index n and the friction coefficient

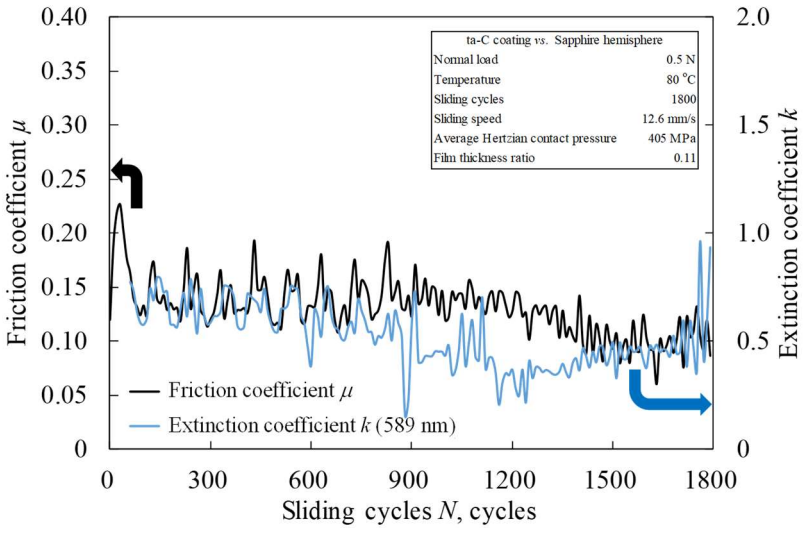

Fig. 12 Evolution of the extinction coefficient k and the friction coefficient

To ensure the repeatability of the friction test, especially the periodical fluctuation of the friction coefficient and the state of the tribofilm at the initial stage of the test, we conducted a new friction test using the same friction conditions as shown in Fig. 9. Figures 13 to 15 show the relationships between the friction coefficient and the thickness, the refractive index n at a wavelength of 589 nm, and the extinction coefficient k at a wavelength of 589 nm, respectively. Figures 13 to 15 show the same trends as in Figs. 9, 11, and 12, respectively. The verification experiment under the same friction conditions supported that increasing the tribofilm thickness was significant for reducing the friction coefficient. In addition, the transition of the tribofilm thickness was also accompanied by changes in the optical properties of the tribofilm; the refractive index n increased but the extinction coefficient k decreased when the friction coefficient decreased.

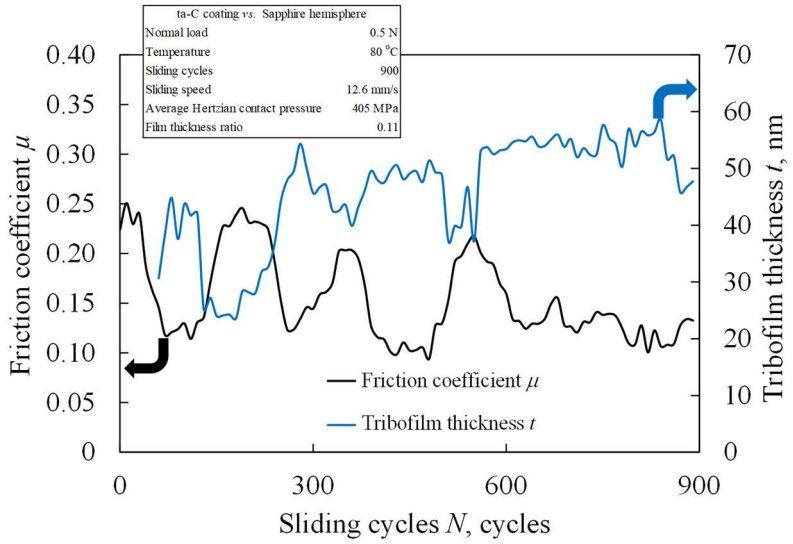

Fig. 13 The evolution of the relationship between the thickness of MoDTC-derived tribofilm and the friction coefficient in the verification experiment

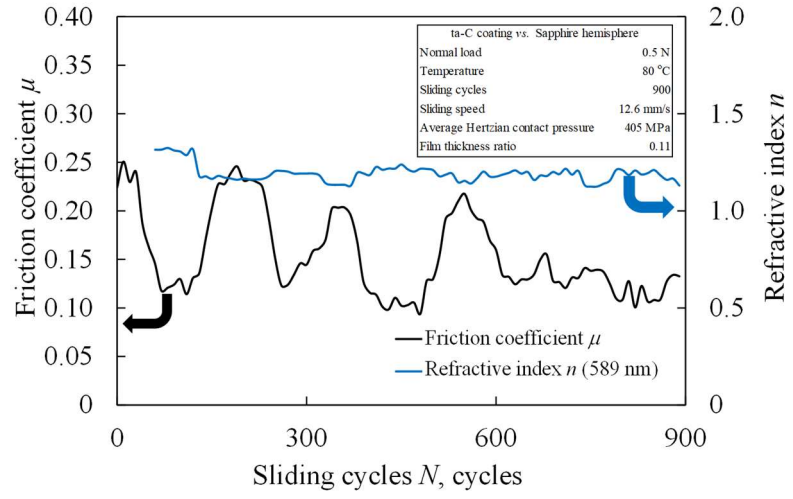

Fig. 14 Evolution of the refractive index n and the friction coefficient of the verification experiment

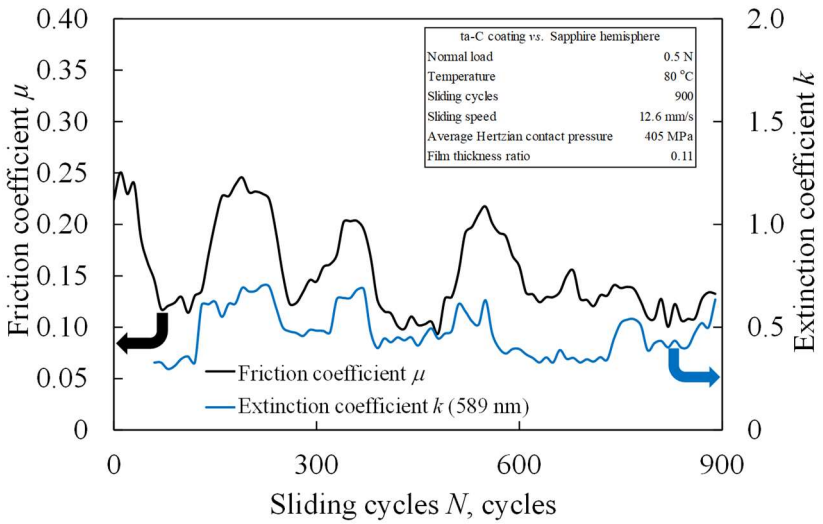

Fig. 15 Evolution of the extinction coefficient k and the friction coefficient of the verification experiment

To confirm the reliability of the optical model for the friction test for the MoDTC-added lubricant, we also confirmed the transformed layer from the as-deposited ta-C coating. We fixed the optical properties of the transformed layer using the result of the pure PAO4 friction test for well convergence. We reconducted the reflectance fitting for some data with a variable parameter of the transformed layer. As a result, the refractive index n and extinction coefficient k of the transformed layer converged to within a difference of 0.01 compared with the value before the recalculation. This recalculation supported the reliability of our analysis method.

Figures 9 and 13 indicate that the tribofilm maintained a thickness of at least 25 nm, meaning that the deeper position of the tribofilm was not easily removed. It is well known that tribofilm composition changes depending on the depth position due to competitive adsorption. From the result of the *in situ* reflectance observation of tribofilm thickness, we considered that a harder and supportive layer existed in the deeper position of the tribofilm and then contributed to maintaining a thickness of more than 25 nm. In addition, the soft and low-shear chemical substances on the topmost surface helped to reduce the friction coefficient (Fig. 16). From the analysis of the reflectance spectroscopy, the thickness and optical properties of the tribofilm fluctuated as the coefficient of friction changed. The optical properties (refractive index n and extinction coefficient k) were original to each tribological product. Therefore, the transition of the tribofilm's optical properties indicated the transition of the tribofilm composition qualitatively. Among the MoDTC-derived products, the refractive index of MoS_2 is 0.6 higher and the extinction coefficient is 0.9 lower than those of Mo_2C. Therefore, the increase in the ratio of MoS_2 and the decrease in the ratio of Mo_2C in the tribofilm caused an increase in the refractive index and a decrease in the extinction coefficient of the overall tribofilm. From the result of the reflectance fitting, we consider that the soft, low-shear layer that contained a larger ratio of MoS_2 formed on the topmost surface. The formation and removal of the soft, low-shear layer caused

fluctuations in both the thickness and the optical properties of the tribofilm. In the next section, we conduct a surface analysis to evaluate the mechanism underlying these effects.

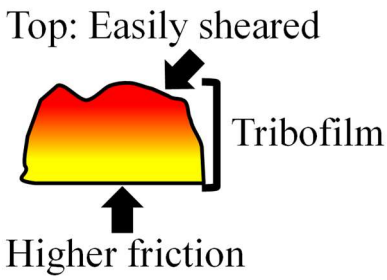

Fig. 16 Schematic model of the MoDTC-derived tribofilm on ta-C coating

5. XPS analysis of the tribofilm and comparison with the *in situ* observation results

We analyzed the tribofilm composition using XPS. The experimental and data fitting conditions were described in section 2.4. We obtained the depth profile using Ar-ion sputtering before each XPS measurement. We measured XPS at three different depths with Ar-ion sputtering times of 12 s, 42 s, and 72 s. The 12 s sputtering elucidated the nature of the topmost surface of the tribofilm due to the removal of the pollution layer on the surface. Figures 17 to 19 show the results of the peak deconvolution of Mo3d peaks with Ar-ion sputtering times from 12 to 72 s, respectively. Figure 20 shows the ratio of Mo compounds in the tribofilm. We focused on the ratio of Mo^{4+}, which indicated the presence of MoS_2. The ratio of Mo^{4+} at the topmost surface was 45.2%. The value decreased to 36.4% at the deeper position (42 and 72 s sputtering times in Fig. 20). This result indicated that a large amount of MoS_2 existed at the topmost surface. In other words, the topmost surface had higher lubricity than the lower layer. We also conducted the peak deconvolution of S2p peaks. Figures 21 to 23 show the results of the peak deconvolution of the S2p peak with Ar-ion sputtering times of 12, 42, and 72 s, respectively. Figure 24 shows the ratio of the bindings state of sulphur. The ratio of the Mo-S bindings at the topmost layer was 90.3% of all bindings of sulphur. In addition, at the deeper position of the tribofilm, the ratios of Mo-S bonding were reduced to 71.3% and 58.6% (42 s and 72 s sputtering times, respectively). The results of S2p peak deconvolution showed the generation of MoS_2 in the MoDTC-derived tribofilm, especially at the topmost layer. We consider that the ratio of MoS_2 at the topmost layer is larger than that at the deeper position from the Mo3d peak deconvolution. The result of the S2p peak deconvolution showed the same trend, which supports the proposed mechanism.

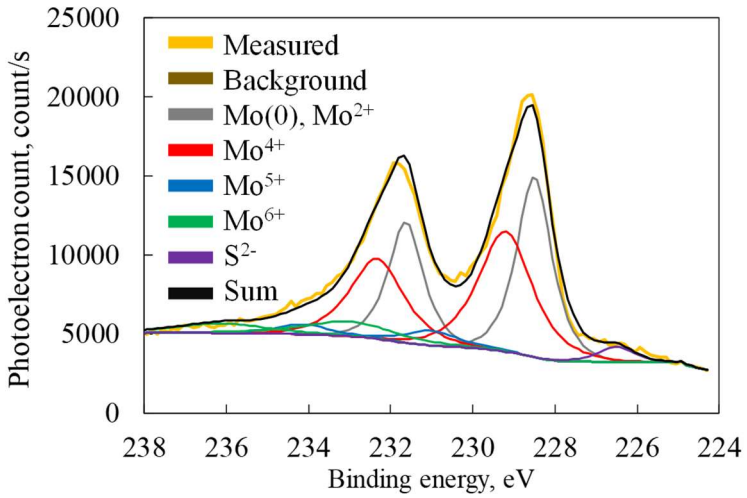

Fig. 17 Result of the peak deconvolution of Mo3d peaks with an Ar-ion sputtering time of 12 s (the topmost layer of the tribofilm)

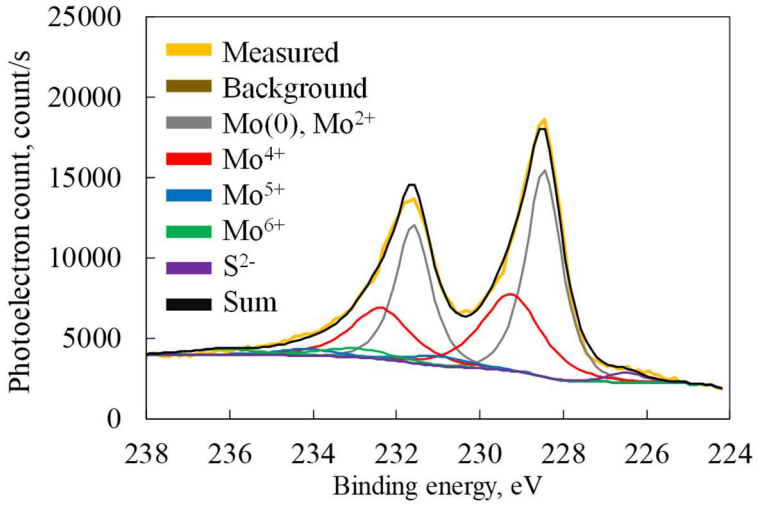

Fig. 18 Result of the peak deconvolution of Mo3d peaks with an Ar-ion sputtering time of 42 s

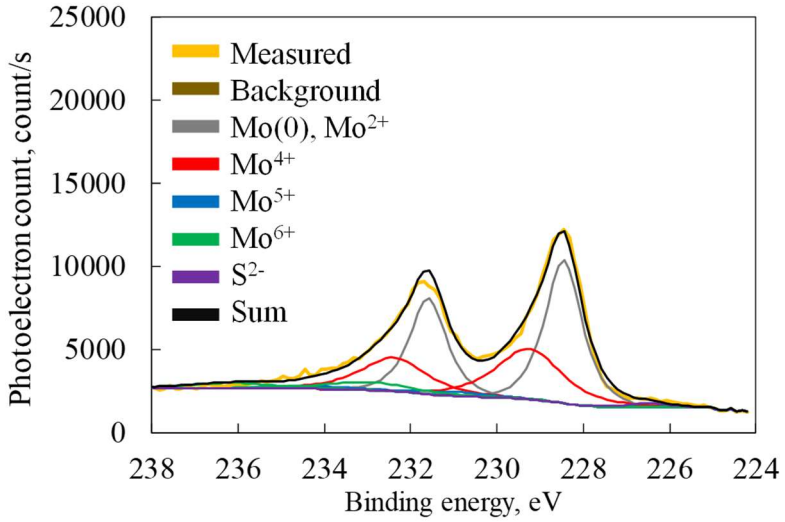

Fig. 19 Result of the peak deconvolution of Mo3d peaks with an Ar-ion sputtering time of 72 s

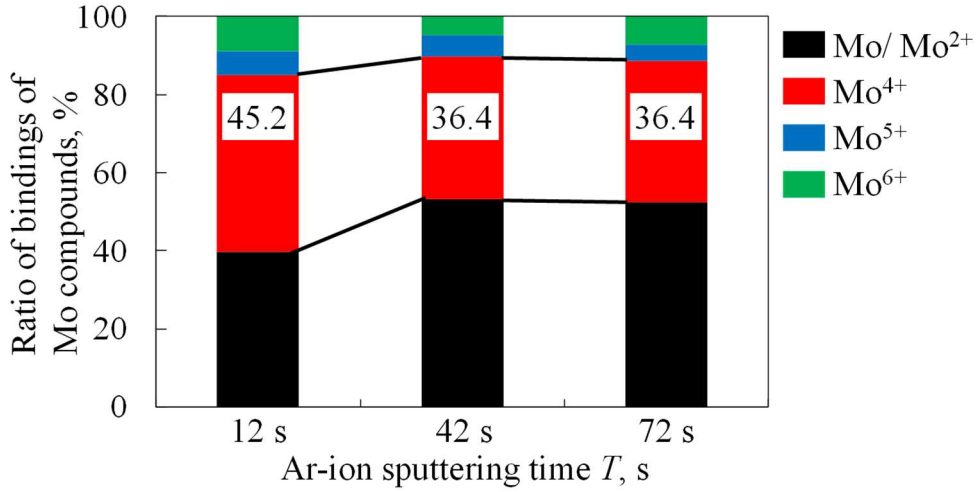

Fig. 20 Ratios of Mo compounds at different depths in MoDTC-derived tribofilm

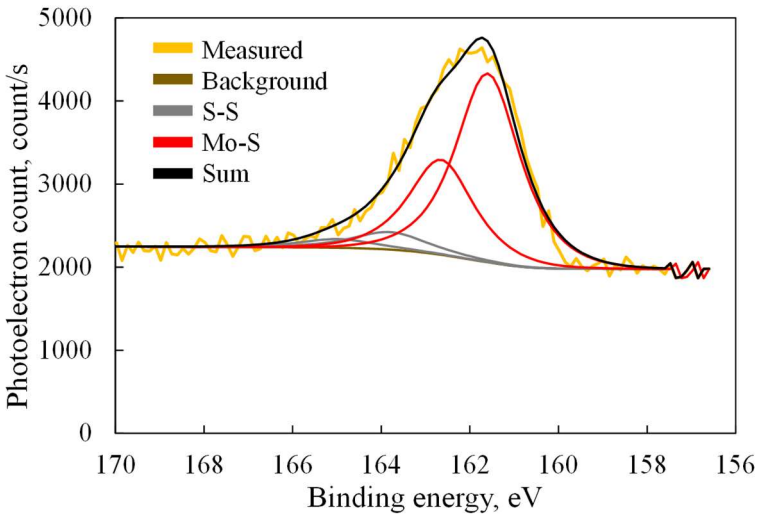

Fig. 21 Result of the peak deconvolution of S2p peaks with an Ar-ion sputtering time of 12 s (the topmost layer of the tribofilm)

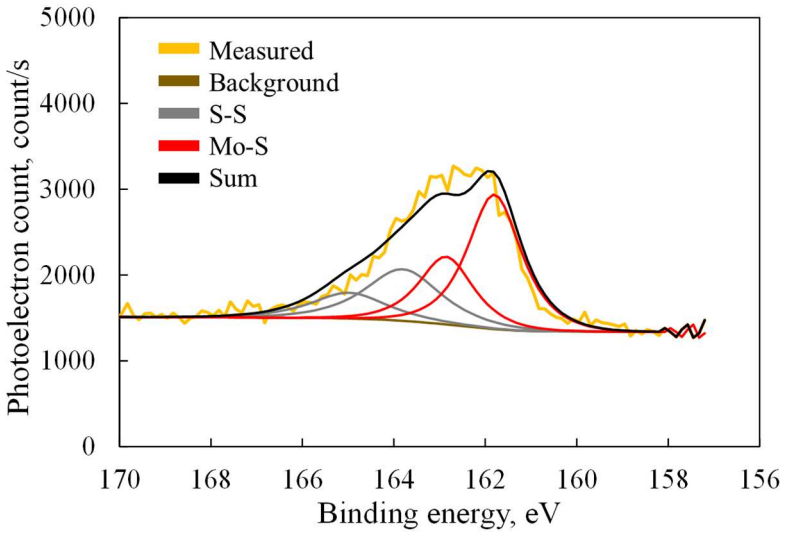

Fig. 22 Result of the peak deconvolution of S2p peaks with an Ar-ion sputtering time of 42 s

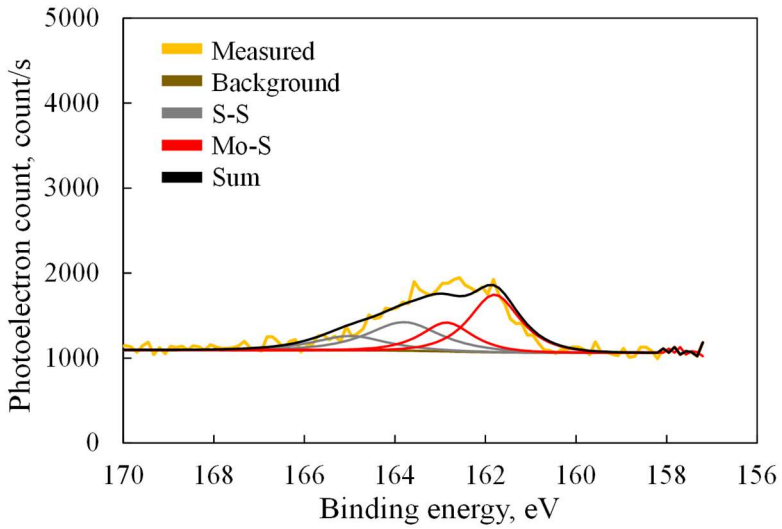

Fig. 23 Result of the peak deconvolution of S2p peaks with an Ar-ion sputtering time of 72 s

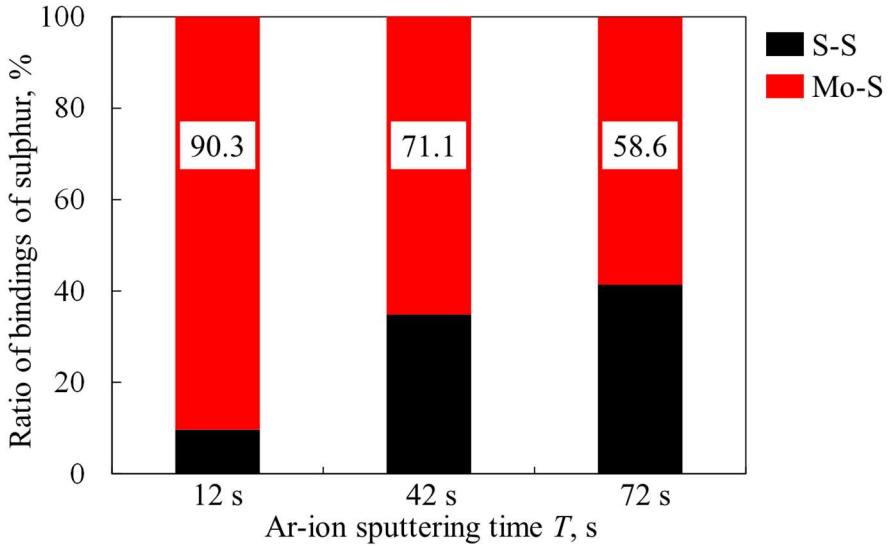

Fig. 24 Ratios of bindings of sulphur at different depths in MoDTC-derived tribofilm

Kassim et al. have reported that Mo_2C is harder than other products from MoDTC [10]. From the XPS analysis of the tribofilm, the topmost layer was considered to be soft and to have high lubricity compared with the deeper position. This is because the ratio of hard Mo_2C on the topmost surface was smaller but the ratio of high-lubricity MoS_2 was larger than that in the deep position. On the other hand, the larger amount of Mo_2C in the deeper position prevented the complete removal of the tribofilm. Komori et al. have conducted friction tests of DLC coatings with different roughnesses or hardnesses under MoDTC- and ZnDTP-containing lubricants [38,39]. When they used rough or hard DLC coatings, the additive-derived tribofilms had large amounts of MoS_2, and then the friction coefficients decreased compared to those with the smooth DLC coatings.

They considered that the generation of MoS_2 requires greater energy than the generation of other MoDTC-derived products (e.g., Mo_2C). Therefore, the use of rough or hard DLC coatings contributed to the increase in the contact pressure and provided more energy, resulting in the increase in MoS_2. Considering these previous works, the hard tribofilm containing a large amount of Mo_2C was first formed on the ta-C coating. Subsequently, the relatively soft and high-lubricity tribofilm, which included more MoS_2, formed on the topmost surface of the tribofilm.

In conclusion, the XPS analysis provided clear evidence that the MoS_2 richly existed on the topmost surface of the tribofilm compared to the deeper position. Interestingly, this result is consistent with the proposed model in Fig. 16 based on the reflectance measurement. The developed *in situ* observation technique enabled us to see the unique formation behavior of the MoDTC-derived tribofilm on the ta-C coating. From the combination of *in situ* reflectance observation and *ex situ* XPS analysis of the tribofilm, we found that the relatively hard tribofilm enhanced the formation of the soft and high-lubricity tribofilm. The formation and removal of the soft layer on the topmost surface affected the fluctuation of the tribofilm. These results should provide a better understanding of tribofilm formation on DLC coatings and thus benefit industrial applications.

6. Conclusions

In the present paper, we clarified the friction characteristics of MoDTC-derived tribofilm on a ta-C coating. DLC coatings (e.g., ta-C) are being applied to many tribocomponents in industrial applications, especially in the automotive industry. On the other hand, some researchers have shown that additives in lubricant oil perform poorly on DLC coatings compared to their performance on metal components. Therefore, a deep understanding of the formation of tribofilm is important. The unique *in situ* observation technique using reflectance spectroscopy on the sliding surface revealed the behavior of tribofilm formation in relation to the friction coefficient.

We conducted friction tests and compared the friction coefficients of MoDTC-added lubricant and pure base oil. At the initial 180 cycles, the friction coefficient in the MoDTC-added lubricant was reduced by 8.4% compared to that in the pure base oil. This indicated that the friction reduction effect of MoDTC emerged at an early stage of the friction test. In addition, at the last 180 cycles, MoDTC decreased the friction coefficient more significantly. The friction coefficient in the MoDTC-added lubricant was approximately 40% lower than that in the base oil.

We analyzed the *in situ* observed reflectance and then calculated changes in thickness of the tribofilm. Especially in the initial stage of the friction test, when the thickness decreased, the friction coefficient increased simultaneously. From the beginning to the end of the friction test, there was a negative correlation between the tribofilm thickness and the friction coefficient. This indicated that their correlation coefficient R was -0.732, a relatively strong relationship. In addition, the nature of the MoDTC-derived tribofilm was evaluated by optical properties (i.e., refractive index and extinction coefficient). Interestingly, an increase in the refractive index was strongly consistent with a decrease in the friction coefficient and an increase in thickness. Optical properties (refractive index n and extinction coefficient k) were unique to each tribological product. Therefore,

the transition of the optical properties of the tribofilm indicated the transition of the composition of the tribofilm qualitatively. Hence, it was indicated that the low friction state had not only the thick tribofilm but also the low friction MoDTC-derived material (i.e., MoS_2).

The XPS analysis provided clear evidence of the different nature of the tribofilm on the topmost surface. Ar-ion sputtering provided a depth profile of the Mo-derived compounds in the tribofilm. As a result, the ratio of Mo^{4+} (most of Mo^{4+} exists as MoS_2) decreased with depth. The topmost surface of the tribofilm had a Mo^{4+} ratio of 45.2%. The value decreased to 36.4% when the Ar-ion sputtering times were 42 s and 72 s. In addition, we conducted the peak deconvolution of the S2p peak. In the topmost surface, 90.3% of sulphur consisted of Mo-S binding, which supported the rich existence of MoS_2. However, the ratios of Mo-S binding decreased to 71.3% and 58.6% (42 s and 72 s sputtering times, respectively). In conclusion, the rich MoS_2 tribofilm on the topmost surface reduced the friction due to its lubricity. On the other hand, there was less MoS_2 in the deep position of the tribofilm, resulting in a higher friction coefficient.

In the present paper, we clarified the relationships between tribofilm thickness, chemical composition, and friction coefficient by combining *in situ* and *ex situ* analyses. The results revealed the unique tribofilm-formation behavior on a ta-C coating, including fluctuations in the thicknesses and optical properties of the tribofilm consistent with changes in the friction coefficient. From the reflectance fitting, we found that the periodical fluctuation of the friction coefficient was synchronized to the transitions in both the thickness and optical properties of the tribofilm. These results brought a new understanding of the friction reduction process in MoDTC-derived tribofilm. From the result of the *in situ* observation, we developed a tribofilm-formation model in which a soft and high-lubricity layer was generated on a hard and supportive underlayer. Finally, the results of the *ex situ* XPS analysis supported that model, indicating the usefulness of *in situ* reflectance observation of tribofilm formation on a ta-C coating.

Declaration of competing interest

The authors declare that they have no known competing financial interests or personal relationships that could have appeared to influence the work reported in this paper.

CRediT authorship contribution statement

Naoya Hashizume: Methodology, Investigation, Writing – original draft. **Motoyuki Murashima:** Investigation, Project administration, Writing – original draft. **Noritsugu Umehara:** Conceptualization, Project administration, Resources, Supervision, Writing – review & editing. **Takayuki Tokoroyama:** Methodology, Writing – review & editing. **Woo-Young Lee:** Methodology, Writing – review & editing.

Acknowledgments

This paper is the result of a collaborative research program with the Research association of Automotive Internal Combustion Engines (AICE) for fiscal year 2020.

References

[1] Ministry of Economy. Trade and Industry of Japan, Automobile energy carrier strategy in Japan. (in Japanese), 2019.

[2] International Energy Agency, Energy technology perspective 2017, 2017.

[3] Holmberg K, Andersson P, Erdemir A. Global energy consumption due to friction in passenger cars. Tribol Int 2012;47:221–34.

[4] Yamamoto Y, Kaneta M. Tribology. Tokyo: Ohmsha Publishing Co. (in Japanese);2010, p. 113-25, 162-9.

[5] Sakate N. Trend of tribology material in automotive engines. Materia Jpn (in Japanese) 2014;12:10-3.

[6] Grossiord C, Varlot K, Martin J, Mogne T Le, Esnouf C. MoS_2 single sheet lubrication by molybdenum. Tribol Int 1999;31:737–43.

[7] Martin JM, Grossiord C, Le Mogne T, Igarashi J. Transfer films and friction under boundary lubrication. Wear 2000;245:107–15.

[8] Espejo C, Wang C, Thiébaut B, Charrin C, Neville A, Morina A. The role of MoDTC tribochemistry in engine tribology performance. A Raman microscopy investigation. Tribol Int 2020;150:106366.

[9] Espejo C, Thiébaut B, Jarnias F, Wang C, Neville A, Morina A. MoDTC tribochemistry in steel/steel and steel/diamond-like-carbon systems lubricated with model lubricants and fully formulated engine oils. J Tribol 2019;141:1–12.

[10] Kassim KAM, Tokoroyama T, Murashima M, Umehara N. The wear classification of MoDTC-derived particles on silicon and hydrogenated diamond-like carbon at room temperature. Tribol Int 2020;147:106176.

[11] Taib MTB, Umehara N, Tokoroyama T, Murashima M. The effect of UV irradiation to a-C:H on friction and wear properties under PAO oil lubrication including MoDTC and ZnDTP. Tribol Online 2018;13:119–30.

[12] Vengudusamy B, Mufti RA, Lamb GD, Green JH, Spikes HA. Friction properties of DLC/DLC contacts in base oil. Tribol Int 2011;44:922–32.

[13] Liu X, Yamaguchi R, Umehara N, Deng X, Kousaka H, Murashima M. Clarification of high wear resistance mechanism of ta-CNx coating under poly alpha-olefin (PAO) lubrication. Tribol Int 2017;105:193–200.

[14] Liu X, Yamaguchi R, Umehara N, Murashima M, Tokoroyama T. Effect of oil temperature and counterpart material on the wear mechanism of ta-CNx coating under base oil lubrication. Wear 2017;390–391:312–21.

[15] Tasdemir HA, Tokoroyama T, Kousaka H, Umehara N, Mabuchi Y. Friction and wear performance of boundary-lubricated DLC/DLC contacts in synthetic base oil. Procedia Eng 2013;68:518–24.

[16] Kano M, Yasuda Y, Ye JP. The effect of ZDDP and MoDTC additives in engine oil on the friction properties of DLC-coated and steel cam followers. Lubr Sci 2004;17:95–103.

[17] Vengudusamy B, Green JH, Lamb GD, Spikes HA. Behaviour of MoDTC in DLC/DLC and DLC/steel contacts. Tribol Int 2012;54:68–76.

[18] Okubo H, Yonehara M, Sasaki S. In Situ Raman Observations of the Formation of MoDTC-Derived Tribofilms at Steel/Steel Contact Under Boundary Lubrication. Tribol Trans 2018;61:1040–7.

[19] Okubo H, Sasaki S. *In situ* raman observation of structural transformation of diamond-like carbon films lubricated with MoDTC solution: Mechanism of wear acceleration of DLC films lubricated with MoDTC solution. Tribol Int 2017;113:399-410.

[20] Xu D, Wang C, Espejo C, Wang J, Neville A, Morina A. Understanding the Friction Reduction Mechanism Based on Molybdenum Disulfide Tribofilm Formation and Removal. Langmuir 2018;34:13523–33.

[21] Murashima M, Yoshino S, Kawaguchi M, Umehara N. Intelligent tribological surfaces: from concept to realization using additive manufacturing. Int J Mech Mater Des 2019;15:757–66.

[22] Murashima M, Imaizumi Y, Murase R, Umehara N, Tokoroyama T, Saito T, et al. Active friction control in lubrication condition using novel metal morphing surface. Tribol Int 2021;156:1–9.

[23] Murashima M, Imaizumi Y, Kawaguchi M, Umehara N, Tokoroyama T. Realization of a Novel Morphing Surface Using Additive Manufacturing and Its Active Control in Friction. J Tribol. 2021;143:1–11.

[24] Nishimura H, Umehara N, Kousaka H, Murashima M. Clarification of effect of transformed layer and oil film on low friction coefficient of CNx coating in PAO oil lubrication by in-situ observation of friction area with reflectance spectroscopy. Tribol Int 2017;113:383–8.

[25] Nishimura H, Umehara N, Kousaka H, Tokoroyama T. Clarification of relationship between friction coefficient and transformed layer of CNx coating by in-situ spectroscopic analysis. Tribol Int 2016;93:660–5.

[26] Okamoto T, Umehara N, Murashima M, Saito K, Manabe K, Hayashi K. The clarification of friction mechanism in oil lubrication for CNx coating by in-situ observation of friction area with reflectance spectroscopy. J Jpn Soc Tribol (in Japanese) 2018;63:755-67.

[27] Okamoto T, Umehara N, Tokoroyama T, Murashima M. The clarification of low friction mechanism in base oil lubrication of ta-CNx coating by in-situ observation with reflectance spectroscopy. Trans JSME (in Japanese) 2019;85:19-00071.

[28] Yamada T, Umehara N, Tokoroyama T, Murashima M, Sato T, Ohara K, Hanyuda K. In-Situ analysis of two phase lubricant oil film with a reflectance spectroscopy. Trans JSME (in Japanese) 2020;86:19-00315.

[29] Fujiwara H, Spectroscopic Ellipsometry. Tokyo: Maruzen Publishing Co. (in Japanese); 2003, p. 5-6, 19, 39-44, 146-4.

[30] Ohara K, Hanyuda K, Kawamura Y, Omura K, Kameda I, Umehara N, et al. Analysis of wear track on DLC coatings after sliding with MoDTC-containing lubricants. Tribol Online 2017;12:110–6.

[31] Moulder JF, Stickle WF, Sobol PE, Bomben KD., Handbook of X-ray Photoelectron Spectroscopy. Waltham: Perkin-Elmer Co.; 1992, p. 40-1, 44-5, 60-1, 65-6, 112-3.

[32] Tohma H. Background removal. J Surf Anal (in Japanese) 2001;8:49-54.

[33] Fukumoto N, Kojima I, Kurahashi M, Shimada H, Nishijima A. Least squares curve fitting in Mo3d X-ray photoelectron spectra for determination of oxidation states of supported molybdenum catalysts. BUNSEKI KAGAKU (in Japanese) 1988;38:65-71.

[34] Kojima I, Fukumoto N, Kurahashi M, Analysis of X-ray photoelectron spectrum with asymmetric Gaussian-Lorentzian mixed function, BUNSEKI KAGAKU (in Japanese) 1986;35:96-100.

[35] Choi JG, Thompson LT. XPS study of as-prepared and reduced molybdenum oxides. Appl Surf Sci 1996;93:143–9.

[36] Peng Y, Meng Z, Zhong C, Lu J, Yu W, Yang Z, et al. Hydrothermal synthesis of MoS_2 and its pressure-related crystallization. J Solid State Chem 2001;159:170–3.

[37] Lahouij I, Vacher B, Martin JM, Dassenoy F. IF-MoS_2 based lubricants: Influence of size, shape and crystal structure. Wear 2012;296:558–67.

[38] Komori K, Umehara N. Effect of surface morphology of diamond-like carbon coating on friction, wear behavior and tribo-chemical reactions under engine-oil lubricated condition. Tribol Int 2015;84:100–9.

[39] Komori K, Umehara N. Friction and wear properties of tetrahedral si-containing hydrogenated diamond-like carbon coating under lubricated condition with engine-oil containing zndtp and modtc. Tribol Online 2017;12:123–34.

[40] Nishioka Y, Probability and Statistics. Tokyo: Ohmsha Publishing Co. (in Japanese); 2013, p. 20-5.